JACS
JOURNAL OF THE AMERICAN CHEMICAL SOCIETY
Article
pubs.acs.org/JACS

Tuning the Ferroelectric Polarization in a Multiferroic Metal–Organic Framework

Domenico Di Sante,*[,†,‡] Alessandro Stroppa,*[,‡] Prashant Jain,[§] and Silvia Picozzi[‡]

[†]Department of Physical and Chemical Sciences, University of L'Aquila, Via Vetoio, L'Aquila, Italy
[‡]CNR-SPIN, L'Aquila, Italy
[§]Los Alamos National Laboratory, 30 Bikini Atoll Road, Los Alamos, New Mexico 87545-0001, United States

Supporting Information

ABSTRACT: We perform density functional theory calculations on a recently synthesized metal–organic framework (MOF) with a perovskite-like topology ABX_3, i.e., $[CH_3CH_2NH_3]Mn(HCOO)_3$, and predict a multiferroic behavior, i.e., a coexistence of ferroelectricity and ferromagnetism. A peculiar canted ordering of the organic A-cation dipole moments gives rise to a ferroelectric polarization of ~2 $\mu C/cm^2$. Starting from these findings, we show that by choosing different organic A cations, it is possible to tune the ferroelectric polarization and increase it up to 6 $\mu C/cm^2$. The possibility of changing the magnitude and/or the canting of the organic molecular dipole opens new routes toward engineering ferroelectric polarization in the new class of multiferroic metal–organic frameworks.

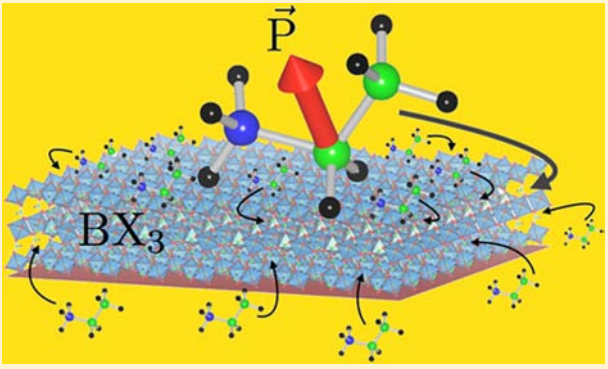

INTRODUCTION

The coexistence of two or more ferroic orders in the same material, such as electric and magnetic ordering, i.e., multiferroicity, has attracted a lot of interest in the past decade.[1] Most of the known multiferroics are inorganic compounds.[2] However, in recent years, the search for new ferroelectrics and multiferroics has been extended to include purely organic compounds.[3,4] A combination of these two classes of materials has opened a new route to achieve multiferroicity, e.g., by considering hybrid organic–inorganic compounds such as metal–organic frameworks (MOFs).[5−15]

MOFs are porous crystalline materials made up of inorganic and organic building blocks, whose cavities can be filled by organic cations.[16] They have been intensively studied for a number of applications such as gas storage, catalysis, molecular recognition, drug delivery, and other medical applications.[17−20] This wide range of applications is a result of their dual nature, namely benefiting from the characteristics of both the inorganic and organic building blocks. For magnetic MOFs, it is possible to control the nature of magnetic coupling due to the variety of possible metal ions, short-ligands, coligands, templates, or even radical ligands carrying a spin degree of freedom.[21] MOFs with perovskite ABX_3 architecture are particularly interesting because some of them show a hydrogen-bonded-related multiferroic behavior.[6,7] The perovskite topology also represents a similarity to the inorganic materials, to which most known multiferroics belong.

A new series of ABX_3 MOFs such as $[C(NH_2)_3][X(HCOO)_3]$, where X = Mn, Fe, Co, Ni, and Cu, have been successfully synthesized.[16] The Cu-based MOF shows a multiferroic and magnetoelectric behavior with an estimated saturated polarization of 0.37 $\mu C/cm^2$.[6] Recently, a novel Cr-based multiferroic and magnetoelectric MOF has also been designed from first-principles. For the first time in the MOF family, a hybrid improper nature of ferroelectricity has been shown, because the coupling of two nonpolar modes induces a polar behavior.[22−28] In the Cr-MOF, at variance with the inorganic case,[22] the coupling of nonpolar distortions is realized by Jahn–Teller pseudorotations[29] and tilting of the molecular A group. The "glue" which mediates this coupling is the hydrogen bonding.[7,30] Interestingly, it has been predicted that a *large* weak-ferromagnetic moment (up to ~1 μ_B/Cr atom) is coupled to the ferroelectric polarization. The latter, however, is still small (~0.22 $\mu C/cm^2$) because it arises from an induced dipole moment on the *nonpolar* A-group organic cation. However, in MOF compounds, it is possible to exploit the large variety of A or X organic groups to tune the multiferroic properties. Here we show how to tune the polarization of ABX_3 type MOFs by carefully choosing the organic A cation.

We performed density functional simulations on a new MOF, $[CH_3CH_2NH_3]Mn[(HCOO)_3]$.[31] Here A is ethylammonium $[CH_3CH_2NH_3]^+$, B is the divalent Mn^{2+} ion, and X is the carboxylate $[HCOO]^-$. Hereafter, we refer to it as the Mn-MOF. We started our calculations from experimental crystallographic data,[32] optimizing the structure until Hellmann–Feynman forces were smaller than 0.02 eV/Å. Kohn–Sham equations were solved using the projector augmented-

Received: August 9, 2013
Published: November 5, 2013

   dx.doi.org/10.1021/ja408283a | J. Am. Chem. Soc. 2013, 135, 18126−18130

wave (PAW) method using the Heyd−Scuseria−Ernzerhof hybrid functional[33] as implemented in VASP.[34,35] The energy cutoff for the plane wave expansion was set to 400 eV; a 3 × 4 × 2 Monkhorst−Pack grid of *k*-points was used. In the Supporting Information (SI), we present systematic convergence tests with respect to energy cutoff and *k*-point sampling. Furthermore, calculations based on different van der Waals functionals are reported to study the effects of weak interactions on the current system. However, no significant differences were found, demonstrating that the main results presented in this study are robust with respect to different approximations used.

STRUCTURAL AND MAGNETIC PROPERTIES

The crystal structure of Mn-MOF is composed of an anionic NaCl-framework of $[Mn^{2+}(HCOO)_3^-]$ where the nearly cubic cavities are occupied and charge-counter-balanced by the ethylammonium $[CH_3CH_2NH_3]^+$ cations. The compound belongs to the polar space group $Pna2_1$, and therefore a spontaneous polarization is allowed by symmetry. Each manganese ion is connected to its six nearest neighbors by bridging ligands. In the lattice, the Mn−HCOO−Mn linkages are along the *c*-axis and along the two diagonal directions of the *ab* plane. The NH_3 and CH_3 groups of the ethylammonium cation form N−H···O and C−H···O hydrogen bonds with the oxygen atoms of the framework. The octahedrally coordinated Mn^{2+} ions (d^5 with $t_{2g}^3e_g^2$ electronic configuration) lie approximately at the center of slightly distorted octahedra with equatorial Mn−O_{eq} bond lengths ranging from 2.17 to 2.23 Å and axial Mn−O_{ax} bond-lengths of 2.17 and 2.22 Å. The octahedra are tilted about the *c*-axis by ∼30°. The Mn-MOF can then be viewed as composed of chains running along the *c*-axis: within each chain, the Mn units are connected by axial $HCO_{ax}O_{ax}$ groups, whereas parallel chains are linked by equatorial $HCO_{eq}O_{eq}$ groups. The Mn sites are coupled antiferromagnetically (AFM) both in the *ab* plane and along the *c*-axis, so that the ground state displays a G-type AFM spin configuration. The magnetic moment associated with each Mn ion is about 4.5 μ_B, consistent with the d^5 electronic configuration. Mapping the system onto a Heisenberg model $H = -\sum_{ij} J_{ij} S_i S_j$, we calculated the intra- and interchain coupling constants $J_c \approx -4$ cm^{-1} and $J_a \approx -8$ cm^{-1} respectively, considering $S_i = \pm 5/2$.

FERROELECTRIC PROPERTIES

It is important to introduce a reference centric structure, in terms of which the low symmetry structure can be described by small amplitude symmetry breaking distortions.[36] In this way, it is possible to analyze atomic displacements responsible of the polarization. In Figure 1a we compare the paraelectric to the ferroelectric phase. As expected, the main atomic displacements involve the organic A groups as shown by oval lines, while very small distortions affect the octahedra (see curved arrow). Note that the A-group cation is polar due to the presence of polar bonds. In fact, the C−N bond is polar because the electronegativity of C and N are 2.6 and 3.0, respectively.[37] Also the N−H bonds are polar (H has 2.2 as electronegativity).[37] Simple geometrical consideration shows that the moments do not compensate, leaving a dipole moment mainly along the C−N bonds. Explicit calculation for the isolated cation gives a dipole moment of 0.78 eÅ. (We consider the isolated A cation in a box of 25 × 25 × 25 Å^3. Convergence

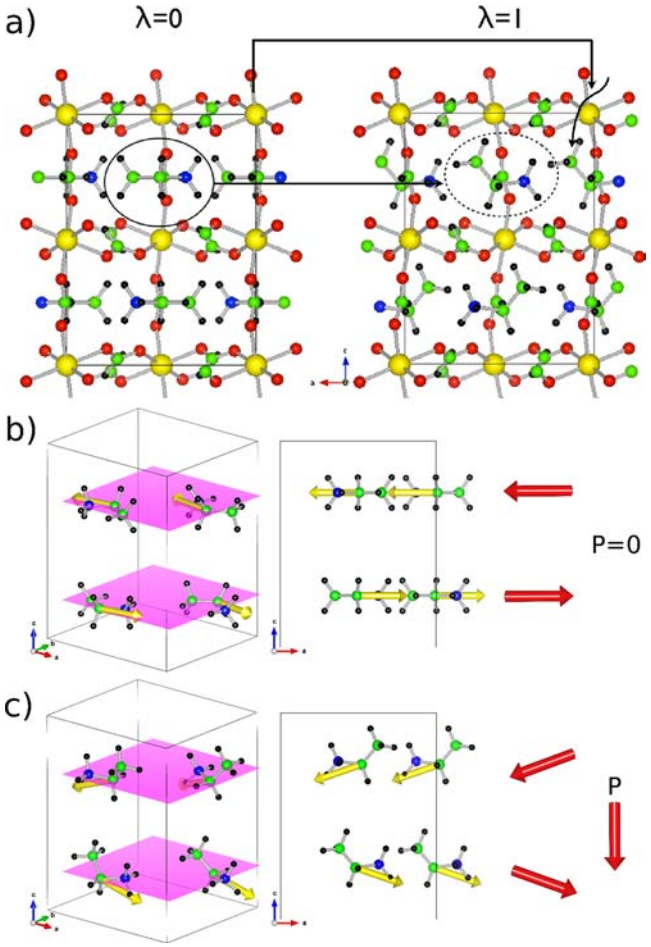

Figure 1. (a) Ball-and-stick model of Mn-MOF in the centric ($\lambda = 0$) (left) and polar ($\lambda = 1$) (right) phases. Most important polar distortions are highlighted by closed lines and arrows. Yellow, red, green, blue, and black balls refer to manganese, oxygen, carbon, nitrogen, and hydrogen atoms, respectively. (b) Spatial ordering of the A-group dipole moments in the centric structure: by symmetry, they are parallel to the *ab* plane and antiparallel on nearest planes along the *c*-axis leading to a zero net polarization. (c) Same as b but in the polar structure: dipole moments do not compensate anymore along *c*-axis because of molecular bending.

with respect to box's dimensions has been carefully checked.) In the centric structure ($\lambda = 0$), the A group is constrained to have the C−C−N bonds in the *ab* plane. In particular, the A-group dipole moments belong to planes parallel to the *ab* plane as shown in Figure 1b: within each plane, there is weak ferroelectric ordering, which is coupled antiferroelectrically with the nearest planes. The resulting polarization is therefore zero (see Figure 1b). In the polar phase ($\lambda = 1$), the ethylammonium molecules is bent out of the *ab* planes, i.e., the C−C−N bond tilts (see Figure 1c). The resulting weak-ferroelectricity is not compensated anymore along the *c* axis and a net dipole moment arises (see Figure 1c). The polar phase is found more stable than the centric one by about 0.38 eV/(f.u.) formula unit.

It is possible to decompose the polar distortion according to symmetrized atomic displacements.[36] In Figure 2 we show the atomic displacement field for the different symmetry modes on top of the centric structure (see arrows). Because the modes act independently on different Wyckoff positions (WPs) of the high-symmetry structure, we can decompose the global

dx.doi.org/10.1021/ja408283a | J. Am. Chem. Soc. 2013, 135, 18126−18130

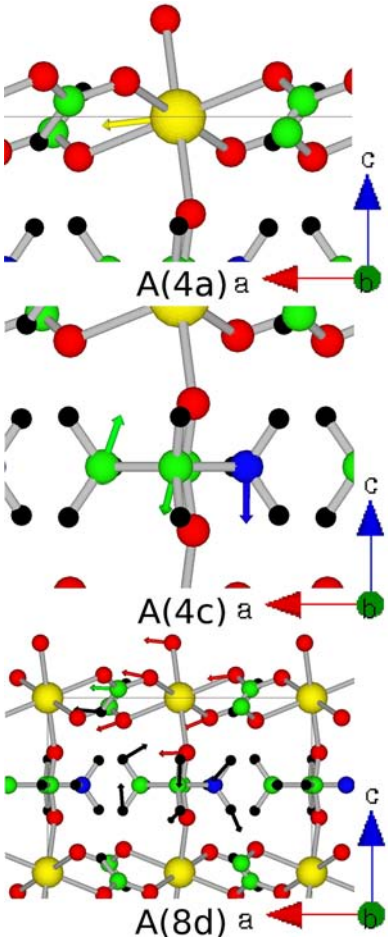

Figure 2. Displacement patterns (arrows) connecting centric to polar structures for atoms belonging to specified Wyckoff positions (4a, 4c, and 8d from top to bottom) for Mn-MOF.

distortion into contributions according to the different WPs orbits.[36] There are three polar contributions, namely A(4a), A(4c), and A(8d), whose largest amplitude is localized on manganese ions, on part of the A groups, and on the octahedral frameworks, respectively (see Figure 2 from top to bottom). For each of them we have calculated the polarization by displacing only the atoms belonging to a given WP orbit and keeping the rest of them in their centrosymmetric positions, thus obtaining $\boldsymbol{P}_{4a}$ = (0,0,−0.37), $\boldsymbol{P}_{4c}$ = (0,0,2.08), and $\boldsymbol{P}_{8d}$ = (0,0,−3.61) μC/cm^2. Notably, their sum, $\boldsymbol{P}_{4a+4c+8d}$ = (0,0,−1.90) μC/cm^2, is almost equal to the total polarization calculated from the total polar distortion, thus approximately retaining a linear behavior. It is possible to decompose the total polarization according to the different functional units of the MOF, such as the A cation, B, and X ligand. The largest contribution comes from the tilting of the A groups inside the cavities of the perovskite, with a net dipole moment of $\mathbf{P}_A$ = (0,0,−2.66) μC/cm^2. Non-negligible contributions come from the X ligands which contribute with an opposite dipole $\mathbf{P}_{X3}$ = (0,0,1.48) μC/cm^2), as well as from the B ions with a contribution $\mathbf{P}_B$ = (0,0,−0.37) μC/cm^2. The induced polar distortions are derived from the X groups due to the coupling via hydrogen bondings. By summing the partial contributions, a total polarization $\mathbf{P}_{A+B+X3}$ = (0,0,−1.55) μC/cm^2 is obtained, again, almost equal to the one calculated using the total polar distortion, $\mathbf{P}_{ABX3}$ = (0,0,−1.64) μC/cm^2, thus retaining a linear behavior.

A-GROUP ENGINEERING

Since the A-group organic cation is the main contributor to the total polarization, we performed computational experiments by considering different organic cations. Starting from the ethylammonium $[NH_3CH_2CH_3]^+$, we considered N and H substitution by P and F atoms, respectively. (As for phosphines that we proposed as possible cations, they are known for their toxicity, volatility, and instability. Despite this, the aim to find a rationale to enhance the ferroelectric polarization in multiferroic MOF justifies their use in our computer simulations.) These atomic modifications will not change dramatically the overall geometry of the molecular cation, as shown in ref 38. Therefore, we consider the series of hypothetical A_iBX_3 MOFs where A_i = $[NH_3CH_2CH_3]^+$, $[PH_3CH_2CH_3]^+$, $[NH_3CH_2CF_3]^+$, $[PH_3CH_2CF_3]^+$, i = 1,...,4. The change of the electronegativity of the constituent atoms causes a charge redistribution with a concomitant change of dipole moment D,[38] which increases according to $D_1 < D_2 < D_3 < D_4$. It is important to mention that the polarizations of the corresponding A_iBX_3 for i = 1,...,4 show almost the same trend, i.e., an increase of the dipole moment in the *isolated* organic cation is accompanied by an increase of the ferroelectric polarization in the corresponding crystal. This is summarized in Figure 3 (top panel), where we show the

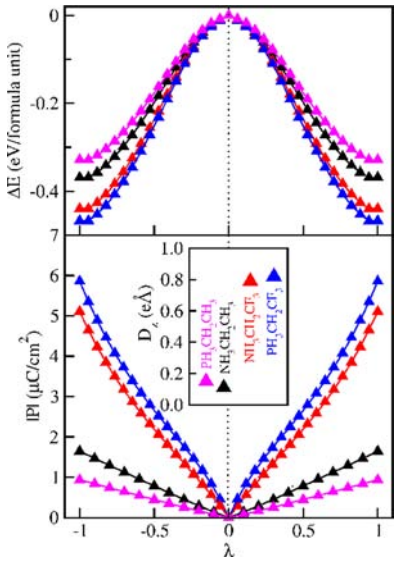

Figure 3. Top panel: Variation of total energy as a function of the normalized amplitude of the polar distortion between centric (λ = 0) and polar (λ = ±1) configurations for MOF crystals with different polar molecules as A group. Bottom panel: Ferroelectric polarization as a function of λ and (in the inset) out-of-plane component D_z of the molecular dipole moment (i.e., the projection along the c polar axis). It is evident that a positive correlation exists between D_z and ferroelectric properties of MOFs. The same trend is found when considering the module of molecular dipoles.

variation of the total energy from the centric to the polar structure. The double-well energy profile characteristic of a switchable ferroelectric system is found in all cases. In Figure 3 (inset of bottom panel), we report $D_{i,z}$ for i = 1,...,4. The minimum value is found for $[NH_3CH_2CH_3]^+$ and the largest for $[PH_3CH_2CF_3]^+$. In the same figure, we also show the MOF polarization as a function of the polar distortion. As expected,

dx.doi.org/10.1021/ja408283a | J. Am. Chem. Soc. 2013, 135, 18126−18130

the largest value of the polarization (as high as ~6 $\mu C/cm^2$) is found for ABX_3 with $A_4 = [PH_3CH_2CF_3]^+$. However, a small deviation is found for A_1 and A_2: although the cation dipole moment follows $D_1 < D_2$, the polarizations of the corresponding A_iBX_3 MOFs for $i = 1, 2$ show the opposite order. This highlights the importance of further polarization effects coming from the framework which contributes to the overall polarization in the MOF. This is evident here because D_1 is very close to D_2.

In summary, starting from a recently synthesized ABX_3 MOF, (i) we predicted a multiferroic behavior with a ferroelectric polarization as high as ~2 $\mu C/cm^2$. (ii) By symmetry mode analysis, it is shown that the organic A cation is the main "actor" of the estimated polarization, because it carries an intrinsic dipole moment. (iii) The net polarization in the crystal is due to the relative canting of the molecular dipole moments with respect to the BX_3 framework, i.e., weak-ferroelectric polarization. (iv) Last, but not least, the possibility of tuning the magnitude and/or the canting of the organic molecular dipole opens new routes to engineering ferroelectric polarization in the new class of multiferroic MOFs.

Finally, we would like to comment on further possible directions to increase ferroelectricity in multiferroic MOFs. Here we have shown the importance of the intrinsic dipole moment of the A-group cation, as well as the relative canting of the corresponding dipolar moment with respect to the framework. It is possible that strain and/or pressure may have a *strong* influence on the dipole moment canting and, therefore, may significantly change the ferroelectric polarization in MOFs. For instance, *in-plane compressive strain could enhance the polarization*. This is obviously important for thin films based on dense MOFs, which is currently a much less developed field. The sensitivity of polarization to applied strain is also found in standard inorganic compounds, but here the effect could be by far larger. Indeed, it has been recently reported that ABX_3 MOF compounds have interesting mechanical properties, such as the possibility of applying an elastic strain up to 5−8% (substantially larger than what is found for typical oxide perovskites), highlighting the potential of the flexible framework to undergo large relaxations in response to local structural changes.[39] Furthermore, the synthesis of perovskite MOFs with smaller distances between magnetic atoms would lead to higher magnetic ordering transition temperatures and to a significant coupling among strain, ferroelectric polarization, and magnetism. In our opinion, these are future directions to explore, from both theoretical and experimental sides.

■ ASSOCIATED CONTENT

Ⓢ Supporting Information

Additional information as noted in the text. This material is available free of charge via the Internet at http://pubs.acs.org.

■ AUTHOR INFORMATION

Corresponding Author

domenico.disante@aquila.infn.it; alessandro.stroppa@spin.cnr.it

Notes

The authors declare no competing financial interest.

■ ACKNOWLEDGMENTS

The work is supported by the MIUR-FIRB project RBAP117RWN. We acknowledge support from SPIN-CNR SEED project PAQSE001 Metal−Organic Frameworks, New Routes to Multiferroicity and Magnetoelectricity. We acknowledge that the results in this paper have been achieved using the PRACE Research Infrastructure resource FERMI based in Italy at CINECA-Bologna under grant agreement MEMOIR-Multiferroic and magnetoElectric Metal OrganIc Frameworks of the fifth PRACE Regular Call for Proposals. We also thankfully acknowledge the computer resources from MareNostrum, technical expertise, and prompt assistance provided by the Spanish Supercomputing Network (RES) and the Barcelona Supercomputing Center. A.S. and D.D.S. thanks Prof. M. Aschi and Dr. T. Bucko for useful discussions. A.S. greatly thanks Prof. C. J. Fennie, Prof. J. M. Rondinelli, and Prof. V. Zapf for invitations to Cornell, Drexel University, and Los Alamos National Laboratory, respectively, and for useful discussions. A.S. thanks Prof. A. Sayede for the kind invitation to Université d'Artois, Faculté des Sciences Jean Perrin, where this work was finalized. P.J. acknowledges the support of the U.S. Department of Energy through the LANL/LDRD Program as well as support of the U.S. National Science Foundation I2CAM International Materials Institute Award, Grant DMR-0844115. The authors greatly acknowledge the careful reading and useful comments by Prof. J. R. Long (University of California, Berkeley). A.S. gratefully acknowledges Prof. A. K. Cheetham and Dr. Wei Li for the invitation to Cambridge University (Functional Inorganics and Hybrid Materials group) and for useful discussions. A.S. thanks Prof. M. H. Whangbo for the warm hospitality at Department of Chemistry, North Carolina State University, and for interesting discussions.

■ REFERENCES

(1) Cheong, S.-W.; Mostovoy, M. *Nat. Mater.* **2007**, *6*, 13.
(2) Khomskii, D. *Physics* **2009**, *2*, 20.
(3) Horiuchi, S.; Tokunaga, Y.; Giovannetti, G.; Picozzi, S.; Itoh, H.; Shimano, R.; Kumai, R.; Tokura, Y. *Nature* **2010**, *463*, 789.
(4) Fu, D.-W.; Cai, H.-L.; Liu, Y.; Ye, Q.; Zhang, W.; Zhang, Y.; Chen, X.-Y.; Giovannetti, G.; M. Capone, J. L.; Hiong, R.-G. *Science* **2013**, *339*, 425.
(5) Ramesh, R. *Nature* **2009**, *461*, 1218.
(6) Stroppa, A.; Jain, P.; Barone, P.; Marsman, M.; Perez-Mato, J. M.; Cheetham, A. K.; Kroto, H. W.; Picozzi, S. *Angew. Chem., Int. Ed.* **2011**, *50*, 5847.
(7) Jain, P.; Ramachandran, V.; Clark, R. J.; Zhou, H. D.; Toby, B. H.; Dalal, N. S.; Kroto, H. W.; Cheetham, A. K. *J. Am. Chem. Soc.* **2009**, *131*, 13625.
(8) Cui, H.; Wang, Z.; Takahashi, K.; Okano, Y.; Kobayashi, H.; Kobayashi, A. *J. Am. Chem. Soc.* **2006**, *128*, 15074.
(9) Gabuda, S. P.; Kozlova, S. G.; Samsonenko, D. G.; Dybtsev, D. N.; Fedin, V. P. *J. Phys. Chem. C* **2011**, *115*, 20460.
(10) Xu, G.-C.; Zhang, W.; Ma, X.-M.; Chen, Y.-H.; Zhang, L.; Cai, H.-L.; Wang, Z.-M.; Xi, R.-G.; Gao, S. *J. Am. Chem. Soc.* **2011**, *133*, 14948.
(11) Fu, D.; Zhang, W.; Cai, H.-L.; Zhang, Y.; Ge, J.-Z.; Xiong, R.-G.; Huang, S. D.; Nakamura, T. *Angew. Chem., Int. Ed.* **2011**, *50*, 11947.
(12) Ahmad, M.; Das, R.; Lama, P.; Poddar, P.; Bharadwaj, P. K. *Cryst. Growth Des.* **2012**, *12*, 4624.
(13) Pardo, E.; Train, C.; Liu, H.; Chamoreau, L.-M.; Dkhil, B.; Boubekeur, K.; Lloret, F.; Nakatani, K.; Tokoro, H.; Ohkoshi, S.; Verdaguer, M. *Angew. Chem., Int. Ed.* **2012**, *51*, 8356.
(14) Zhang, W.; Xiong, R. *Chem. Rev.* **2012**, *112*, 1163.
(15) Liu, B.; Shang, R.; Hu, K.; Wang, Z.-M.; Gao, S. *Inorg. Chem.* **2012**, *51*, 13363.
(16) (a) Hu, K. L.; Kurmoo, M.; Wang, M.; Gao, S. *Chem.—Eur. J.* **2009**, *15*, 12050. (b) Wang, W.; Yan, L. Q.; Cong, J. Z.; Zhao, Y. L.; Wang, F.; Shen, S. P.; Zou, T.; Zhang, D.; Wang, S. G.; Han, X. F.; Sun, Y. *Sci. Rep.* **2013**, *3*, 2024−1. (c) Sanchez-Andujar, M.; Presedo,

S.; Yanez-Vilar, S.; Castro-Garcia, S.; Shamir, J.; Senaris-Rodriguez, M. *Inorg. Chem.* **2010**, *49*, 1510. (d) Bauer, E. M.; Bellitto, C.; Colapietro, M.; Portalone, G.; Righini, G. *Inorg. Chem.* **2003**, *42*, 6345. (e) Nénert, G.; Adem, U.; Bauer, E. M.; Bellitto, C.; Righini, G.; Palstra, T. T. M. *Phys. Rev. B* **2008**, *78*, 054443. (f) Polyakov, A. O.; Arkenbout, A. H.; Baas, J.; Blake, G. R.; Meetsma, A.; Caretta, A.; van Loosdrecht, P. H. M.; Palstra, T. T. M. *Chem. Mater.* **2012**, *24*, 133. (g) Canadillas-Delgado, L.; Fabelo, O.; Rodriguez-Velamazán, J. A.; Lemee-Cailleau, M.-H.; Mason, S. A.; Pardo, E.; Lloret, F.; Zhao, J.-P.; Bu, X.-H.; Simonet, V.; Colin, C. V.; Rodríguez-Carvajal, J. *J. Am. Chem. Soc.* **2012**, *134*, 19772. (h) Canepa, P.; Chabal, Y. J.; Thonhauser, T. *Phys. Rev. B* **2013**, *87*, 094407. (i) Canepa, P.; Nijem, N.; Chabal, Y. J.; Thonhauser, T. *Phys. Rev. Lett.* **2013**, *110*, 026102. (j) Wang, Z. X.; Jain, P.; Choi, K. Y.; van Tol, J.; Cheetham, A. K.; Kroto, H. W.; Koo, H. J.; Zhou, H.; Hwang, J. M.; Choi, E. S.; Whangbo, M. H.; Dalal, N. S. *Phys. Rev. B* **2013**, *87*, 224406.
(17) Férey, G.; Cheetham, A. K. *Science* **1999**, *283*, 1125.
(18) Férey, G.; Mellot-Draznieks, C.; Serre, C.; Millange, F.; Dutour, J.; Surblé, S.; Margiolaki, I. *Science* **2005**, *309*, 2040.
(19) Cheetham, A. K.; Rao, C. N. R. *Science* **2007**, *318*, 58.
(20) Rao, C. N. R.; Cheetham, A. K.; Thirumurugan, A. *J. Phys.: Condens. Matter* **2008**, *20*, 083202.
(21) Demir, S.; Zadrozny, J. M.; Nippe, M.; Long, J. R. *J. Am. Chem. Soc.* **2012**, *134*, 18546.
(22) Benedek, N. A.; Fennie, C. J. *Phys. Rev. Lett.* **2011**, *106*, 107204.
(23) Bousquet, E.; Dawber, M.; Stucki, N.; Lichtensteiger, C.; Hermet, P.; Gariglio, S.; Triscone, J.-M.; Ghosez, P. *Nature* **2008**, *452*, 732.
(24) Fukushima, T.; Stroppa, A.; Picozzi, S.; Perez-Mato, J. M. *Phys. Chem. Chem. Phys.* **2011**, *13*, 12186.
(25) Mulder, A.; Benedek, N.; Rondinelli, J.; Fennie, C. *Adv. Funct. Mater.* **2013**, *23*, 4810.
(26) Rondinelli, J.; Fennie, C. J. *Adv. Mater.* **2012**, *24*, 1961.
(27) Rondinelli, J. M.; Spaldin, N. *Adv. Mater.* **2011**, *23*, 3363.
(28) Ghosez, P.; Triscone, J. *Nat. Mater.* **2011**, *10*, 269.
(29) Bersuker, I. B. *Chem. Rev.* **2013**, *113*, 1351.
(30) Stroppa, A.; Barone, P.; Jain, P.; Perez-Mato, J.; Picozzi, S. *Adv. Mater.* **2013**, *25*, 2284.
(31) Wang, Z.; Zhang, B.; Otsuka, T.; Inoue, K.; Kobayashi, H.; Kurmoo, M. *Dalton Trans.* **2004**, 2209−2216.
(32) The Royal Society of Chemistry, http://www.rsc.org/suppdata/dt/b4/b404466e/.
(33) Heyd, J.; Scuseria, G. E.; Ernzerhof, M. *J. Chem. Phys.* **2003**, *118*, 8207.
(34) Kresse, G.; Furthmüller, J. *Phys. Rev. B* **1996**, *54*, 11169.
(35) Paier, J.; Marsman, M.; Hummer, K.; Kresse, G.; Gerber, I. C.; Ángyán, J. G. *J. Chem. Phys.* **2006**, *124*, 154709.
(36) Stroppa, A.; Di Sante, D.; Horiuchi, S.; Tokura, Y.; Vanderbilt, D.; Picozzi, S. *Phys. Rev. B* **2011**, *84*, 014101.
(37) Periodic Table of Elements, http://www.webelements.com/.
(38) Weaver, R.; Parry, R. W. *Inorg. Chem.* **1966**, *5*, 718.
(39) (a) Li, W.; Zhang, Z.; Bithell, E. G.; Batsanov, A. S.; Barton, P. T.; Saines, P. J.; Jain, P.; Howard, C. J.; Carpenter, M. A.; Cheetham, A. K. *Acta Mater.* **2013**, *61*, 4928. (b) Tan, J. C.; Civalleri, B.; Lin, C.-C.; Valenzano, L.; Galvelis, R.; Chen, P.-F.; Bennett, T. D.; Mellot-Draznieks, C.; Zicovich-Wilson, C. M.; Cheetham, A. K. *Phys. Rev. Lett.* **2012**, *108*, 095502. (c) Kosa, M.; Tan, J. C.; Merrill, C. A.; Krack, M.; Cheetham, A. K.; Parrinello, M. *Chem. Phys. Chem.* **2010**, *11*, 2332. (d) Li, W.; Probert, M. R.; Kosa, M.; Bennett, T. D.; Thirumuragan, A.; Burwood, R. P.; Parrinello, M.; Howard, J. A. K.; Cheetham, A. K. *J. Am. Chem. Soc.* **2012**, *134*, 11940. (e) Li, W.; Barton, P. T.; Kiran, M. S. R. N.; Burwood, R. P.; Ramamurty, U.; Cheetham, A. K. *Chem.—Eur. J.* **2011**, *17*, 12429. (f) Li, W.; Kiran, M. S. R. N.; Manson, J.; Schlueter, J. A.; Thirumurugan, A.; Ramamurty, U.; Cheetham, A. K. *Chem. Commun* **2013**, *49*, 4471. (g) Tan, J.-C.; Jain, J.; Cheetham, A. K. *Dalton* **2012**, *41*, 3949.